very low value of $\phi = 0.004$ brittlelike fracture was observed. At the higher value of 0.02 a well-defined neck appeared, which upon subsequent deformation traveled through the entire specimen. For $\phi = 1$ essentially homogeneous deformation was observed, whereas $\phi = 0.1$ represents an intermediate case between homogeneous deformation and necking. In the latter case multiple micronecks were formed.

It was already noted above that the morphologies generated with the model are unrealistically porous in highly deformed regions. And it was explained[13] that this is a direct consequence of the simplification (to save computer time) that the specimen was contracted along the x axis by the square root of the overall draw ratio, instead of local draw ratio. The latter, of course, may differ widely from the overall draw ratio, particularly in materials with a low value of ϕ. This discrepancy is clearly illustrated in Figure 5b,c.

For purpose of comparison, micrographs of actual samples of solution-crystallized UHMW PE are presented in Figure 6. This figure displays photographs of polyethylene films of $M_w = 1.5 \times 10^6$ and $M_n \sim 2 \times 10^5$ crystallized from respectively 0.5, 2, and 10% v/v solutions in Decalin and from the melt (see ref 19 for experimental details); the latter three samples were drawn to a macroscopic draw ratio of approximately 3 at 100 °C. The resemblance between these micrographs and the "calculated morphologies" of Figure 5 is truly remarkable. It illustrates that the present model indeed is capable of handling the very complex issue of connecting events on molecular level to macroscopic properties and features.

Acknowledgment. We thank Dr. S. R. Allen for many stimulating discussions and Dr. E. J. Roche for producing the optical micrographs.

Registry No. PE, 9002-88-4.

References and Notes

(1) Termonia, Y.; Smith, P. *Macromolecules* **1987**, *20*, 835.
(2) Ward, I. M. *Mechanical Properties of Solid Polymes, 2nd ed.*; Wiley: New York, 1983.
(3) Smith, P.; Lemstra, P. J. to Stamicarbon, B. V. (DSM), U.S. Patent 4 344 908, 1982; U.S. Patent 4 430 383, 1983.
(4) In contrast to studies based on the affine deformation principle, the importance of the initial distribution of orientations along the deformation axis here is of little importance. Indeed, in the present approach, that distribution is destroyed already in the early stages of the deformation process after a few van der Waals bond breakings or slippage events have occurred (see below).
(5) Meirovitch, H. *J. Phys. A: Math. Gen.* **1982**, *A15*, L735; *J. Chem. Phys.* **1983**, *79*, 502.
(6) See, e.g., the review in: Kausch, H. H. *Polymer Fracture*; Springer-Verlag: Berlin, 1978; Chapter IV.
(7) Smith, P.; Lemstra, P. J.; Booij, H. C. *J. Polym. Sci., Polym. Phys. Ed.* **1981**, *19*, 877.
(8) Treloar, L. R. G. *The Physics of Rubber Elasticity*, 2nd ed.; Clarendon: Oxford; 1985.
(9) Flory, P. J. *Statistical Mechanics of Chain Molecules*; Interscience: New York, 1969; p 12.
(10) Kauzmann, H.; Eyring, H. *J. Am. Chem. Soc.* **1940**, *62*, 3113.
(11) Termonia, Y.; Meakin, P.; Smith, P. *Macromolecules* **1985**, *18*, 2246; *Ibid* **1986**, *19*, 154.
(12) During that process the end-to-end vectors of chain strands are prohibited to contract below their equilibrium length corresponding to the random coil configuration.
(13) This calculation is an oversimplification that ignores the fact that locally the draw ratios may be very large indeed, and this procedure thus undercompensates for contractions along the x axis. This leads to too large distances between the chains in the x direction and to too "open" a morphology (see later). This simplification, which amounts to an important saving in computer time, is justified because the principal axis of interest in the present work is the y axis.
(14) Porter, R. S.; Johnson, J. F. *Chem. Rev.* **1966**, *66*, 1.
(15) Graessley, W. W. *Adv. Polym. Sci.* **1974**, *16*, 58.
(16) Mackley, M. R.; Solbai, S. *Polymer* **1987**, *28*, 1115.
(17) In the paper of ref 7, where relation 9 originally was proposed, the factor $3^{1/2}$ was erroneously omitted (see ref 18).
(18) Kramer, E. J. *Adv. Polym. Sci.* **1983**, *52/53*, 33.
(19) Smith, P.; Lemstra, P. J.; Pijpers, J. P. L.; Kiel, A. M. *Colloid Polym. Sci.* **1981**, *259*, 1070.

Effect of Chain Association on the Viscosity of Dilute Ionomer Solutions

Fumihiko Tanaka

Laboratory of Physics, Faculty of General Education, Tokyo University of Agriculture and Technology, Fuchu-shi, Tokyo 183, Japan. *Received September 24, 1987; Revised Manuscript Received December 21, 1987*

ABSTRACT: Ionic groups attached at wide intervals along nonpolar polymer chains produce strong associating interactions in solution. This paper presents a general theory to infer the detailed structure of chain aggregates from the experimental data on the solution viscosity of ionomers in nonpolar solvents. In the limit of low concentration, equilibrium dimensions of an intramolecular network formed by ionic interaction are estimated as a function of χ (the solvent–monomer interaction parameter) and ϵ (strength of the bonding energy). For higher polymer concentrations, cluster distribution function of intermolecular aggregates is obtained through multiple-equilibria conditions. It is shown that their geometrical structure is characterized by two exponents, q and ν, giving interchain connectivity and fractal dimensionality, respectively. The result is compared with the recent experimental measurements on sodium sulfonated polystyrene in cyclohexanone.

I. Introduction

Flexible long-chain molecules containing a small fraction of strongly associating chemical groups are known to exhibit several unusual solution properties. For example, the incorporation of relatively low levels of ionic groups onto the backbone structure of a polymer chain profoundly changes the rheological properties of these solutions as compared to its nonionic counterpart. These changes are caused to a large extent by the formation of intra- and intermolecular cross-links due to the mutual association of the ionic groups.

Recent experimental studies[1-3] have explored the solution viscosity of polymers such as sulfonated polystyrene ionomers or ethylene–propylene terpolymers over wide

0024-9297/88/2221-2189$01.50/0

range of polymer concentration in a number of organic solvents. In a dilute regime, for example, it was found[1] that ion pair interaction induces strong intra- and interchain association of sodium sulfonated polystyrene (SPS) in solvents of low polarity such as cyclohexanone (CH) or tetrahydrofuran (THF), while classical polyelectrolyte behavior dominates the ion pair association in polar solvents such as dimethyl sulfoxide or dimethylformamide.

In this paper, attention will be paid mainly to the effect of ionic association on the solution viscosity of a model metal sulfonated ionomer dissolved in nonpolar solvents. Experimental measurements[1] on SPS/CH showed that the reduced viscosity markedly diminishes as the sulfonate level is increased in the limit of low polymer concentration, while it sharply increases in higher concentrations. Such unusual behavior may be attributed to the following facts:

(1) In the limit of infinite dilution, intrachain cross-linking dominates. Each polymer shrinks through network formation, and the effective hydrodynamic radius of the region, into which solvent flow cannot penetrate, diminishes.

(2) As the concentration increases, intermolecular association prevails. The spatial regions contained in the aggregates rapidly grow, and since they exclude the external flow, viscosity increases more substantially than the case where the polymer chains are separated from one another. At a certain concentration eventually the system becomes macroscopically connected and turns into gel.

The influence of association on the reduced viscosity of macromolecules in dilute solution was theoretically considered by Wolf et al.[4] A general scheme was developed to relate cluster distribution of aggregates to the reduced viscosity. The association constants governing multiple equilibria were, however, not derived from the microscopic interaction between reacting monomers. Comparison with experimental observation was therefore beyond the scope of that study. Mechanism of shear thickening by flow-induced association was considered by Witten and Cohen.[5] An intuitive argument was presented on the balance between intra- and interchain association for various flow rates. Cates and Witten[6] also considered chain conformation in networks formed by associating polymer chains. Since both theories were confined to qualitative arguments, however, a detailed test of them by comparison with experimental observations was not sufficient.

The purpose of this paper is to construct a statistical mechanical theory for the analysis of macromolecular aggregates and to evolve a standard procedure for the estimation of the aggregation parameters from the reduced viscosity versus concentration curve. We elucidate the spatial structure and size distribution of the aggregates and reveal how they exert influence on the solution viscosity.

II. Theory

Considering the fact that the experimental results are fairly well reproducible for the case of the solvents of lower polarity such as CH or THF, it is apparent that these solutions do achieve thermodynamic equilibrium at modest ionic levels. There are, however, many cases where equilibrium is not achieved. Specifically, those solutions in which the cations are little solvated (such as xylene for sodium SPS) will be the latter case. Since our theory is based on the equilibrium thermodynamics, it may not apply to the latter nonequilibrium environments.

We consider a system of volume V containing N ionomer chains and N_0 organic solvent molecules. Let n be the degree of polymerization (DP) of a chain, and let us assume that the size a of a monomer is of the same order as that of the solvent molecule. We thus have $V = (N_0 + nN)a^3$. Let N_m be the number of aggregates consisting of m cross-linked polymer chains (hereafter refered to as m-clusters). We then have $\sum_{m=1}^{\infty} mN_m = N$. The total volume fraction ϕ_m of m-clusters in the system is given by $\phi_m = mnN_m/(N_0 + nN)$. The number of m-clusters in a unit volume is given by $C_m = N_m/V = \phi_m/(nma^3)$.

To study solution viscosity, we consider a spatial region for each m-cluster inside which the external solvent flow cannot penetrate. Let $V(m;n)$ be the volume of such region formed by an m-cluster comprized of n chains. The net effect of clustering is to increase this hydrodynamic volume compared to the summation of individual volume in the state where chains are dissolved apart from one another. The total of newly produced hydrodynamic volume contained in a unit volume of the solution is then expressed as

$$\Phi_m = V(m;n)\phi_m/(mna^3) \tag{II.1}$$

Let us introduce the volume fraction $f_m \equiv \phi_m/\phi$ of chains forming m-clusters among all chains, where $\phi \equiv \sum\phi_m = nN/(N_0 + nN)$ is the total volume concentration of the polymer. The polymer weight concentration c is related to ϕ through $c = \rho\phi$ by the use of the density $\rho = M/(nN_Aa^3)$ of the polymer, where M is the molecular weight and N_A is Avogadro's number.

According to a general theory,[7] the specific viscosity η_{SP} defined by $\eta_{SP} \equiv (\eta - \eta_0)/\eta_0$, where η_0 is the solvent viscosity, can be developed in a power series of Φ_m as

$$\eta_{SP} = \kappa\sum_m \Phi_m + \sum_{m,m'} \kappa^{(2)}_{m,m'}\Phi_m\Phi_{m'} + \dots \tag{II.2}$$

where $\kappa = 2.5$ is the Einstein coefficient and $\kappa^{(2)}_{m,m'}$ expresses the strength of hydrodynamic interaction between an m-cluster and an m'-cluster.

We next introduce concept of intrinsic viscosity $[\eta]_m$ for *each* m-cluster. This is defined by the equation

$$[\eta]_m \equiv \kappa\frac{N_A}{mN}V(m;n) \tag{II.3}$$

According to this definition, $[\eta]_1$ is the intrinsic viscosity of an isolated chain. We refer to it simply as $[\eta]$. Eliminating the unknown $V(m;n)$ from eq II.2 by the use of eq II.3 we find

$$\eta_{SP} = (\sum[\eta]_m f_m)c + (\sum(k_H)_{m,m'}[\eta]_m[\eta]_{m'}f_mf_{m'})c^2 + \dots \tag{II.4}$$

where $(k_H)_{m,m'} \equiv \kappa^{(2)}_{m,m'}/\kappa^2$ is the Huggins' constant between a pair of clusters m and m'.

III. Intrinsic Viscosity

Consider the limit of infinite dilution. Though it is probable that there remains some degree of aggregation depending on the cation, solvent quality, and ionic content, we assume that fraction of clusters is small enough for carefully stirred samples. Under this assumption, the distribution function takes the form $f_m = \delta_{m,1}$. The problem is reduced to finding the intrinsic viscosity $[\eta]$ for an isolated chain, or equivalently, the effective hydrodynamic volume $V(1;n)$ of it.

To obtain the hydrodynamic radius of an isolated ionomer chain, let us describe it by a model chain consisting of two kinds of constitutional units. A monomer unit A of one chemical species is reactive and capable of forming a bond with another of the same kind. We call the thus-formed pair a "dimer". The other kind of monomer units are assumed to be nonfunctional. Let the functional monomer be arranged regularly after every train of t nonfunctional monomer units. The number fraction p of A-monomer units is then given by $p = 1/(t + 1)$. Consider

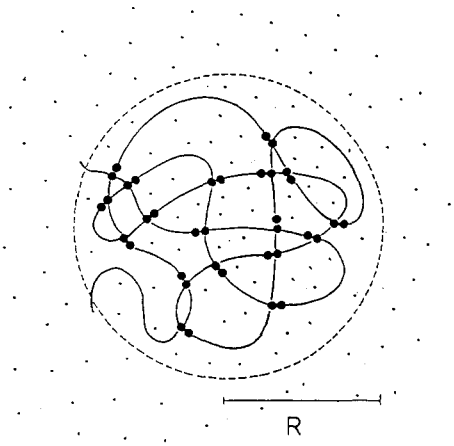

Figure 1. Intramolecular network formed by ion pairing shown in a solvent of temperature T. It is a complete network of functionality 4. The radius of gyration R is considered as a function of ϵ, the bonding energy of pairing, and $\chi(T)$, the solvent–monomer interaction parameter.

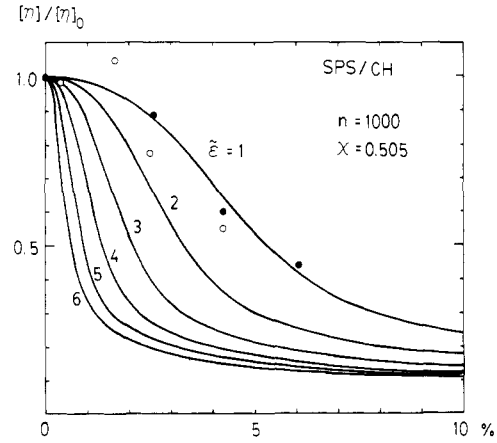

Figure 2. Intrinsic viscosity of SPS chain relative to that of pure PS shown against the sulfonate content. Symbols ○ and ● show the results of experimental measurements for different samples. The dimensionless binding energy $\tilde{\epsilon} \equiv \epsilon/k_BT$ is varied from curve to curve.

that such chain is dissolved in a solvent and in thermal equilibrium. We describe solvent–monomer interaction by the Flory parameter $\chi(T)$ as a function of the absolute temperature T. Some A-monomer units are connected pairwise to form dimers. The total chain can therefore be regarded as a temporal network of segmental chains connected by cross-links of functionality 4 (Figure 1). Due to such intramolecular bridging, the total region occupied by the chain is smaller compared to that of a nonfunctional chain. We assume that the thus-formed network is so dense that it is regarded as a nondraining particle, or equivalently, the hydrodynamic radius is of the order of radius R of gyration of the segment distribution.

We have recently studied[8] the variation of the chain conformation in an intramolecular network formed by a model polymer. Specifically, the radius of gyration was obtained as a function of the temperature and the bonding energy of the reacting pair. Let α be the expansion factor of the polymer chain. This is defined by the ratio of the gyration radius to that of the ideal chain: $\alpha \equiv R/(n^{1/2}a)$. The intrinsic viscosity is expressed as $[\eta] = Kn^{1/2}\alpha^3$ in terms of α, where K is a numerical constant independent of DP. Furthermore let x be the number fraction of dimers among the total number of A monomers. By minimizing the free energy of a chain, our theory[8] derived coupled equations for determining equilibrium values of α and x as a simultaneous function of the parameter $\chi(T)$ and the pairing energy ϵ:

$$\frac{x}{(1-2x)^2} = \frac{p}{2n^{1/2}} e^{4+\tilde{\epsilon}-3\alpha^2} \qquad \text{(III.1a)}$$

$$(1 + 2npx)\alpha^2 - 1 + ng(v) = 0 \qquad \text{(III.1b)}$$

where $\tilde{\epsilon} \equiv \epsilon/k_BT$, $v \equiv 1/n^{1/2}\alpha^3$, and $g(v) \equiv (\ln(1-v))/v + 1 + \chi v$. The parameter v shows volume fraction of a region actually occupied by the polymer segments inside the sphere of radius R. The first equation describes the law of mass action among reacting monomers connected sequentially by a chain. The second assures homogeneity of the chemical potential of a mobile solvent molecule through the dividing surface of radius R.

We have applied the theory to our ionomer system. Figure 2 shows reduction of the intrinsic viscosity of sodium sulfonated polystyrene (SPS) in cyclohexanone (CH). The ratio of $[\eta]$ to that of the pure polystyrene (PS) $[\eta]_0$ is plotted against the sulfonate level p. We have extrapolated the experimental data[1] to infinite dilution and show the results by the symbols ○ and ●. They were obtained from two different samples of the same species. The number-average molecular weight of the backbone PS was estimated to be 106 000, and the weight-average molecular weight 288 000. We have therefore fixed the polymer DP to be 10^3 in our numerical calculation. As detailed information on the χ parameter is not available for PS in cyclohexanone, we assume that it will not be dramatically different from that in cyclohexane. We therefore set $\chi = 0.505$, which is the value for PS dissolved in cyclohexane at room temperature. Results of numerical calculation are shown by curves. The dimensionless pairing energy $\tilde{\epsilon}$ is varied from curve to curve. Agreement between theory and experiment is obtained for $\tilde{\epsilon} = 1$. The effective attraction between sulfonated sodium in the solvent CH, therefore, proved to be comparable to the thermal energy.

IV. Intermolecular Association

As the polymer concentration increases, intermolecular association prevails. To consider the concentration dependence of the solution viscosity, let us introduce a factor $u(m)$ defined by

$$u(m) \equiv \frac{V(m;n)}{mV(1;n)} \qquad \text{(IV.1)}$$

This ratio gives the increment of the hydrodynamic volume due to chain association. The first term of the specific viscosity (eq II.4) can be rewritten as

$$\sum_{m=1}^{\infty} [\eta]_m f_m(\phi) = [\eta]g(c) \qquad \text{(IV.2)}$$

where new function $g(c)$ is defined by

$$g(c) \equiv \sum_{m=1}^{\infty} u(m) f_m(\phi) \qquad \text{(IV.3)}$$

It is regarded as a function of the weight concentration c instead of the volume concentration. As for the second-order term in (III.2) we assume that coupling constant k_H is independent of m and m':

$$(k_H)_{m,m'} = k_H \qquad \text{(IV.4)}$$

This assumption is supported by the fact that the Huggins' constant depends, for most polymer species, only slightly on the molecular weight. As clusters of different size have identical internal structure, hydrodynamic interaction among them may safely be assumed to be identical. The numerical value of k_H is known to be roughly 0.3 for most

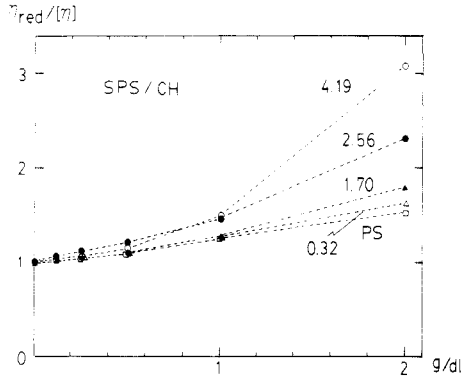

Figure 3. Experimental observation on the reduced viscosity $\eta_{red} \equiv (\eta - \eta_0)/(\eta_0 c)$ of SPS shown against the polymer weight concentration. Sulfonate content p is varied from curve to curve. The viscosity is divided by $[\eta]$ so that each curve starts at unity.

polymers. We will, however, fix it for the PS/CH system by comparing our theory with the experiment.

Under such an assumption for $(k_H)_{m,m'}$, the viscosity–concentration curve of the associating polymer solution may be summarized in the form

$$\eta_{SP}/c[\eta] = g(c) + k_H[\eta]g(c)^2c + \dots \quad \text{(IV.5)}$$

Experimental results[1] of the viscosity curve for SPS/CH system are shown in Figure 3, where $\eta_{SP}/(c[\eta])$ is plotted against the polymer weight concentration c. The sulfonate level is varied from curve to curve. Once we find the cluster distribution $f_m(\phi)$ as a function of the total polymer concentration through multiple equilibrium conditions, together with the volume increment $u(m)$ by the consideration of internal structure of clusters, we will be able to estimate the viscosity curve.

V. Multiple-Equilibria Condition

Let μ_m be the chemical potential of a cluster consisting of m ionomer chains. The condition for association equilibrium is given by the uniformity of the single-chain chemical potential in any size of clusters:

$$\mu_m/m = \text{constant independent of } m \quad \text{(V.1)}$$

As the m-cluster in the solution can be regarded as a macromolecule having mn monomer units, we may apply the lattice theory of polydisperse polymer solutions[9] to our system. The chemical potential takes the form

$$\mu_m = \mu_m^\circ + k_BT\{\ln \phi_m - (mn - 1) + mn(1 - 1/(\langle m\rangle n))\phi + mn\chi(1 - \phi)^2\} \quad \text{(V.2)}$$

where $\langle m\rangle \equiv \phi/(\sum\phi_m/m)$ is the number-average cluster size, and μ_m° the Gibbs free energy of a single m-cluster in the state when it is isolated from the solvent. Condition V.1 then leads to

$$\phi_m = K_m\phi_1^m \quad \text{(V.3)}$$

with the association constant K_m given by

$$K_m = \exp(-\beta m\Delta\tilde{\mu}_m^\circ + m - 1) \quad \text{(V.4)}$$

The free-energy change $\Delta\tilde{\mu}_m^\circ$ of a single chain caused by joining in an m-cluster from the isolated state is defined by

$$\Delta\tilde{\mu}_m^\circ \equiv \mu_m^\circ/m - \mu_1^\circ \quad \text{(V.5)}$$

This is decomposed into two terms: $\Delta\tilde{\mu}_m^\circ = \Delta e_m - T\Delta s_m$, where Δe_m is the energy change and Δs_m the entropy change. As we will show in the following, the energy change may be summarized in the form

$$\beta\Delta e_m = E(m^{-q} - 1) \quad \text{(V.6)}$$

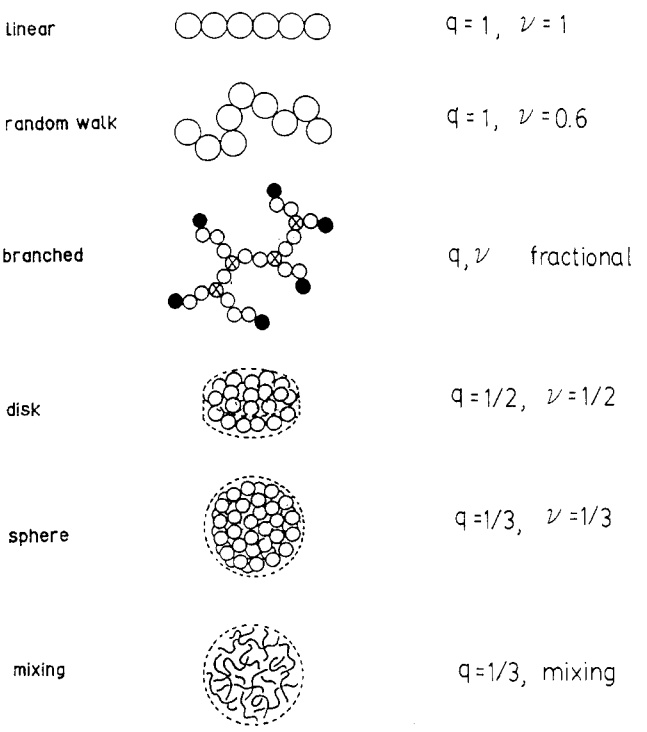

Figure 4. Some typical forms of aggregation are shown together with their indexes. In each part, a circle shows a polymer chain whose internal structure is shown in Figure 1. Polymers on the surface and at junction points are marked in the case of a branched aggregate.

for a wide variety of geometrical constructions of an m-cluster. The constant E is a dimensionless energy gain when a pair of chains are combined in a cluster. The index q characterizes the way chains are connected with each other in an aggregate. As for the entropy change, we set $\Delta s_m = k_B \ln p$ independent of m, since the chance for m cluster network formation is proportional to the logarithm of the number of combinations there are to make pairs among reacting monomers. Hence we have

$$\beta\Delta\tilde{\mu}_m^\circ = E(m^{-q} - 1) - \ln p \quad \text{(V.7)}$$

We next proceed to discuss the volume increment $u(m)$. According to spatial arrangement of m chains in a cluster, the effective hydrodynamic volume is characterized by another index, ν, in the form $V(m;n)/V(1;n) = m^{3\nu}$ and hence

$$u(m) = m^{3\nu-1} \quad \text{(V.8)}$$

The relation is based on the fact that the hydrodynamically inactive region in a cluster is governed by its mass distribution.

Let us illustrate the physical meanings of the two indexes q and ν in more details. Figure 4 shows some possible forms of aggregates. Each small sphere corresponds to an intramolecular network formed by single chain. In the case of rodlike aggregate, which is made up of a linear array of identical chains, the total internal energy E_m of an m-cluster is given by $E_m = -Ek_BT(m - 1)$, where Ek_BT is the binding energy of chain–chain bonding. Hence, we have $\Delta e_m \equiv E_m/m - E_1 = Ek_BT(m^{-1} - 1)$ to find $q = 1$ for a linear aggregate. As for the index ν, $\nu = 1$ is expected for a rodlike case, since the radius of gyration of a rod is proportional to its length. In the case where chains are randomly placed one after another, the backbone of a linear aggregate may be regarded as a random-walk path. One may therefore say that the index q reflects mutual connectivity among constitutional molecules in an aggre-

gate, while ν reflects the spatial distribution of molecular masses.

In the case of an aggregate having many branches as shown by the third figure in Figure 4, similar consideration leads to

$$q = 1 - \lim_{m\to\infty} \{\ln (n_{end}/2 - n_J)/\ln m\} \qquad (V.9)$$

where n_{end} is the number of molecules on the surface of an aggregate and n_J is the number of molecules at internal junction points. We have a fractional value for both q and ν in this case. Recall that $\nu^{-1} \equiv D$ is called the "fractal dimension" of an aggregate in the literature.[10] Similarly it is easy to see $q = \nu = {}^1/_2$ for a closely packed disk and $q = \nu = {}^1/_3$ for a sphere. The effect of index q on aggregate formation has been thoroughly discussed in ref 11. In addition to these forms, there is an important case for a polymeric solution where chains are well interpenetrated with each other in a cluster (see the bottom figure in Figure 4). We have three dimensional connectivity $q = {}^1/_3$ for such a mixed chain assembly. Under the assumption that chain ends in the cluster do not modify the dimensions of segment distribution, the aggregate can be regarded as a single giant network whose structure is decided by the coupled equations presented in section III. Hence we are led to

$$u(m) = m^{1/2}\left\{\frac{\alpha(mn)}{\alpha(n)}\right\}^3 \qquad (V.10)$$

where $\alpha(n)$ is the expansion factor of a network formed by n monomers.

Putting all the results together, we can evaluate the cluster distribution $f_m(\phi)$ and the function $g(c)$ and hence the viscosity–concentration curve.

VI. Results

We start with the problem of how clusters appear as the total polymer concentration increases. The multiple equilibrium condition (eq V.3) explicitly yields

$$\phi = \frac{1}{e}\left\{\frac{x}{pe^E} + \sum_{m=2}^{\infty} x^m \exp(-Em^{1-q})\right\} \qquad (VI.1)$$

where a combined variable $x \equiv pe^{E+1}\phi_1$ has been used in place of the concentration ϕ_1 of isolated chains. Figure 5 shows how x changes against the total concentration for three representative values of q. Since the mole fraction of sodium sulfonate on a chain was varied over the range from 0 to 6% in the experiments,[1] we have fixed p to be 0.05 to see the effect of connectivity index q. Furthermore, since the optimal value of E to fit the experiment on SPS/CH turns out to be slightly above 5 as we will show in the followings, we have adopted $E = 5$ as a typical value for the interchain binding energy. The number of cross-links between two chain molecules is estimated to be roughly 5, because the bonding energy for an ion pair was found as $\tilde{\epsilon} \cong 1$. Hence nearly 5 among the $0.05 \times 10^3 = 50$ ions on a chain are reacting. The fraction of isolated chains gets gradually saturated in the case of one-dimensional connectivity $q = 1$, while it reveals a sharp bend in a narrow range of concentration for lower connectivity $q = {}^1/_2$ and $q = {}^1/_3$. In both of the latter cases, a cluster of infinite size appears[1] above the concentration where sudden change occurs. The concentration at which the increase in the fraction ϕ_1 of isolated chains stops is called the critical micelle concentration (cmc). It is found from the relation V.3. Substituting for K_m the explicit form derived from $\Delta\mu_m°$, we are led to an equation $\phi_m = [p\phi_1 \exp\{E(1 - m^{-q}) + 1\}]^m/e$. The condition $p\phi_1 \exp\{E(1 - m^{-q}) + 1\} \cong 1$ therefore determines the radius of convergence for the power series $\sum\phi_m$. This condition is first satisfied for $m = \infty$, and hence we have

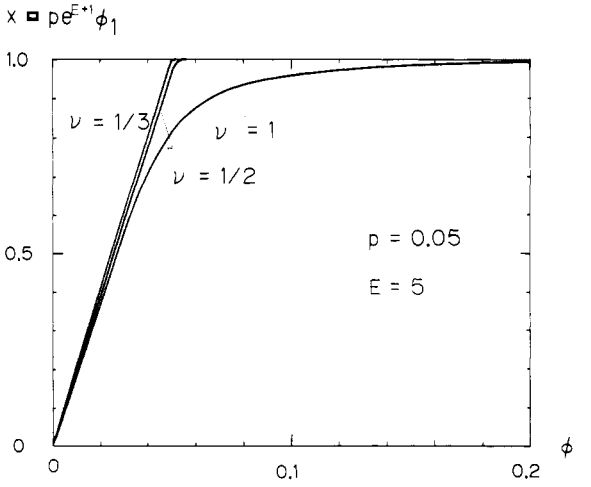

Figure 5. Reduced fraction x of polymers that remain isolated in the system plotted against total volume fraction of the polymer for three values of q.

$$p(\phi_1)_{cmc}e^{E+1} \cong 1 \qquad (VI.2)$$

where $(\phi_1)_{cmc}$ denotes the isolated-chain concentration at the cmc. The volume fraction of m-clusters at the cmc is found to be $\phi_m \cong \exp\{-(Em^{1-q} + 1)\}$. The solution is polydisperse with broad cluster distribution for $q = 1$. In fact it is constant within the approximation VI.2. For smaller values of q, however, the cluster population immediately decreases as the size increases. We have for example $\phi_m \sim e^{-Em^{1/2}}$ for $q = {}^1/_2$ and $\sim e^{-Em^{2/3}}$ for $q = 3$. Since the summation over m of ϕ_m is bounded from above in these cases, the excess quantity $\phi - \sum\phi_m$, if it exists, must be in an infinite cluster. Transition to large macroscopic aggregate occurs above the cmc for q smaller than unity. All of these arguments are quite parallel to those given for the micellization of low molecular weight surfactants.[11] Figure 6 shows the distribution of cluster size at two different concentrations where x is close to unity. Distribution is very broad for $q = 1$ as shown in Figure 6a. Large clusters consisting of several tens of ionomer chains appear as x approaches unity. In contrast, as shown in Figure 6b, only a small amount of tiny clusters is formed for lower values of q even when x is extremely close to unity.

Let us proceed to the g function (eq IV.3). When particularly $\nu = {}^1/_3$ is satisfied as is the case for spherical close packing, $g(c)$ is identically unity, and hence there is no increment in the hydrodynamic volume due to association. In contrast a maximum increment is obtained for the rodlike aggregates for which $\nu = 1$. The fractal dimensionality of aggregates observed in various colloidal systems mostly lies between these extreme limits. The effect of the index ν on the viscosity–concentration curve is shown in Figure 7. Parameters are fixed as was done in the preceding section. The volume fraction has been translated into the weight concentration by the use of the density $\rho = 1.04$ g/cm^3 for PS. The initial slope of the experimental curve for pure PS/CH gives $k_H = 0.356$ for the Huggins' constant. Curves in the figure prove that appearance of aggregates, whose internal region contains a large number of empty spaces to accommodate solvent molecules, can cause a substantial increase in the solution viscosity. It is therefore expected that the better the solvent, the larger the viscosity increment. In fact ex-

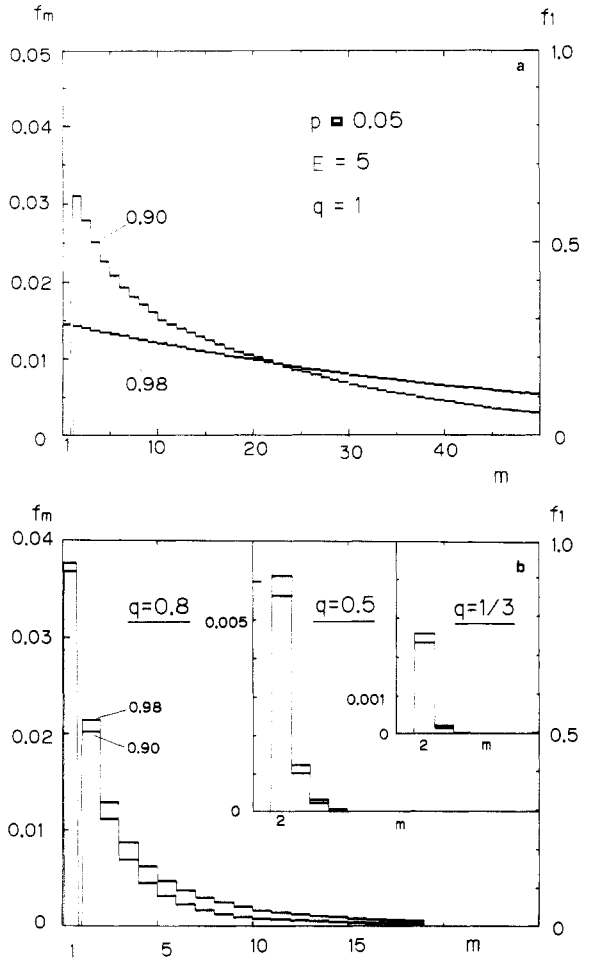

Figure 6. Calculated cluster distribution function near the cmc shown against the cluster size. Figures by the curves stand for the fraction x of isolated chains: (a) $q = 1$; (b) Smaller values of q.

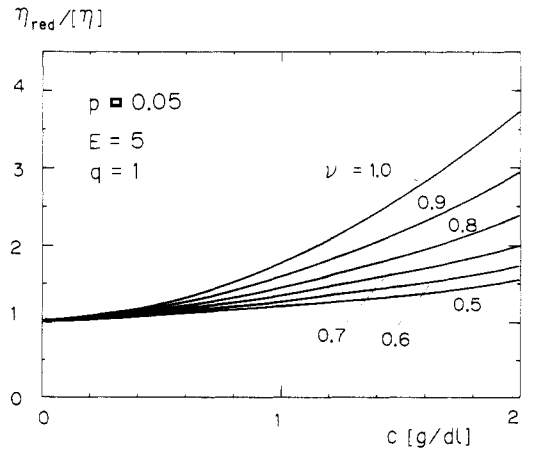

Figure 7. Effect of the index ν on the viscosity–concentration curve shown for $q = 1$.

periment[1] proved that η_{red} for SPS/THF reaches 10 times as large a value as that for pure PS/THF at concentration $c = 2$ g/dL.

Consider next the influence of connectivity index q on the viscosity curve. Geometrical consideration on the two indexes leads to a condition $q \geq \nu$ for physical systems. For example, a cluster with $q = 1$ and $\nu = {}^1/_2$ is a linear array of constitutional polymer chains whose spatial configuration is random-walk-like. A cluster with $q = {}^1/_2$ and $\nu = 0.4$, for another example, is a curved disk whose radius of gyration is smaller than that of a planar disk. Figure 8

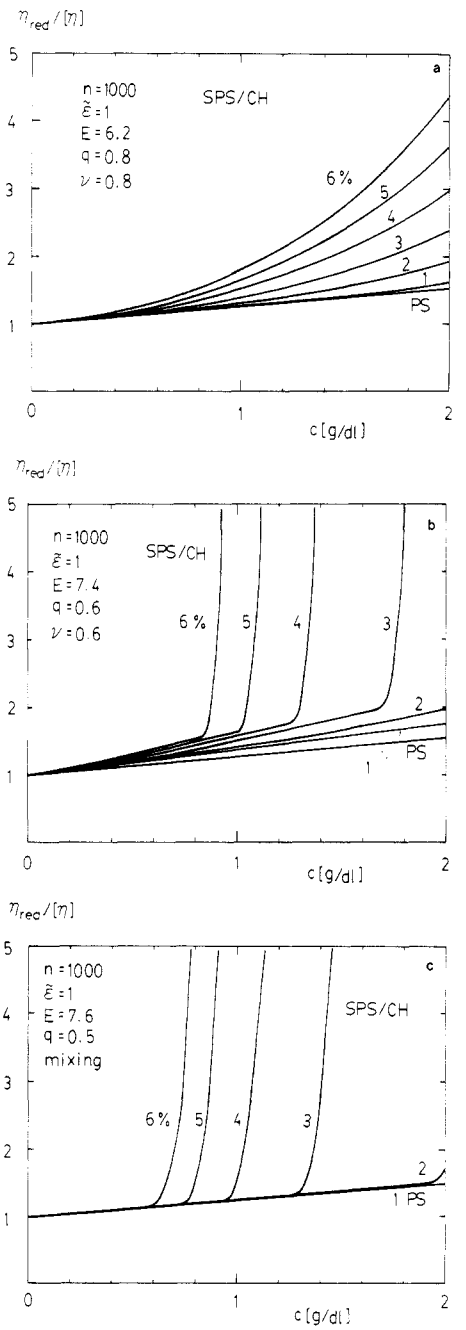

Figure 8. Calculated viscosity–concentration curves. In each figure optimal values of E are found to fit experimental results (Figure 3) for given indexes q and ν: (a) $q = \nu = 0.8$; (b) $q = \nu = 0.6$; (c) $q = 0.5$ mixing.

shows some of the theoretical results. In each figure the optimal value of E is found to fit the experimental observation (Figure 3) for given q and ν. It is clear that the lower the value of q, the sharper the viscosity change. This is caused by the appearance of a sharp cmc for lower values of q. In the case of a cluster in which polymer chains are interpenetrated with each other (mixing case, Figure 8c), the effect of association on the viscosity curve is indistinct until the cmc, while a sudden rise occurs above the cmc. Since a sudden rise has not been observed for SPS in all solvents examined so far, formation of a compact cluster (either small q or mixing) turns out to be improbable in ionomer systems. As far as SPS/CH is concerned, the $q = \nu = 0.8$ case (Figure 8a) agrees very well with the experiments. Since we have two unknown parameters, q and ν, however, it should be noted that the conclusion has not been confirmed to be unique one. It is probable that

another combination of a pair of numerical values for them may produce similar result. Other experimental studies using techniques such as light or neutron scattering will be helpful to fix the indexes directly.

VII. Conclusion and Discussion

We have introduced two indexes to characterize spatial structure of a polymeric aggregate formed in a solution through ionic pairing. A general theory to infer their values from viscosity measurement has been developed on the basis of a multiple-equilibria theory of association. Since the treatment of the viscosity curve in our theory is general enough, it can be applied to another colloidal solutions, including those such as latex in oil or red cells in blood. In the latter system it is well-known that aggregates called *rouleaux* in fact control the blood viscosity through association and dissociation processes. This is an example of a system whose solution viscosity has an absolute meaning in its own right.

Looking at the problem from the rheological point of view, temperature and shear rate dependence of the viscosity can provide extensive clues for understanding the nature of association taking place in ionomer solutions. A series of viscosity–temperature measurements[2] showed that very strong and durable interchain networks were formed and persisted up to 150 °C. It was also proved experimentally[1] that viscosity in Couette flow increased with increasing shear, attained a maximum, and then fell again at higher shear rates. The shear-induced thickening phenomena were understood[5] to be caused by elongation of polymer chains under shear. Elongation might promote reaction between ions on different chains at the expense of associations within a chain. Theoretical studies are required for further quantitative understanding of dynamic properties of associating ionomers.

References and Notes

(1) Lundberg, R. D.; Makowski, H. S. *J. Polym. Sci., Polym. Phys. Ed.* **1980**, *18*, 1821. Lundberg, R. D.; Phillips, R. R. *Ibid.* **1982**, *20*, 1143. Peiffer, D. G.; Lundberg, R. D. *Ibid.* **1984**, *22*, 2051.
(2) Agarwal, P. K.; Makowski, H. S.; Lundberg, R. D. *Macromolecules* **1980**, *13*, 1679. Agarwal, P. K.; Lundberg, R. D. *Ibid.* **1984**, *17*, 1918. Agarwal, P. K.; Lundberg, R. D. *Ibid.* **1984**, *17*, 1928. Agarwal, P. K.; Garner, R. T.; Lundberg, R. D. *Ibid.* **1984**, *17*, 2794.
(3) Kim, M. W.; Peiffer, D. G. *J. Chem. Phys.* **1985**, *83*, 4159. Peiffer, D. G.; Kaladas, J.; Duvdevani, I. *Macromolecules* **1987**, *20*, 1397.
(4) Wolf, C.; Silberberg, A.; Priel, Z.; Layec-Raphalen, M. N. *Polymer* **1979**, *20*, 281.
(5) Witten, T. A., Jr.; Cohen, M. H. *Macromolecules* **1985**, *18*, 1915.
(6) Cates, M. E.; Witten, T. A., Jr. *Macromolecules* **1986**, *19*, 72.
(7) Flory, P. J. *Principles of Polymer Chemistry*; Cornell University Press: Ithaca, NY, 1953; Chapter 14.
(8) Tanaka, F.; Ushiki, H. *J. Chem. Phys.* **1986**, *84*, 5925.
(9) Chapter 12 of ref 7.
(10) *On Growth And Form: Fractal and Non-Fractal Patterns in Physics*; Stanley, H. E., Ostrowsky, N., Eds.; Nijhoff: Hingham, MA, 1986.
(11) Israelachvili, J. N. *Physics of Amphiphiles: Micelles, Vesicles and Microemulsions* Degiorgio, V., Corti, M., Eds.; North-Holland: Amsterdam, 1985; p 24.

Complexation of Stereoregular Poly(methyl methacrylates). 11. A Mechanistic Model for Stereocomplexation in the Bulk

Elwin Schomaker and Ger Challa*

Laboratory of Polymer Chemistry, State University of Groningen, Nijenborgh 16, 9747 AG Groningen, The Netherlands.

Received July 22, 1987; Revised Manuscript Received November 13, 1987

ABSTRACT: The process of stereocomplexation between isotactic and syndiotactic PMMA in the bulk was studied by means of differential scanning calorimetry and wide-angle X-ray scattering as a function of annealing time and temperature. It appeared that in all cases the material obtained was partly crystalline. For low annealing temperatures the samples showed multiple endotherms with different characteristics. A mechanistic model, in which subsequent crystallization of the complexed chain sections plays an important role, is presented which accounts for the observed phenomena. At low annealing temperatures complexation proceeds much faster than subsequent crystallization resulting in a fringed-micellar kind of growth, while at higher annealing temperatures lamellar crystallization occurs directly. The endotherms are interpreted respectively as the decomplexation of complexed sections partly organized into fringed-micellar clusters of complexes (T_m^1) and the simultaneous decomplexation and melting of lamellarly crystallized complexes (T_m^3). Apart from these main endotherms also a small endotherm was found (T_m^2), which was assigned to the decomplexation of complexed sections, formed during scanning. The critical sequence length necessary for complexation and the mobility of the chains, and consequently the annealing temperature and molar mass of the polymers employed, are the most important parameters in the mechanistic scheme presented.

Introduction

Ever since the first report of Fox et al.[1] on mixtures of isotactic (i) and syndiotactic (s) poly(methyl methacrylate) (PMMA) showing crystallinity, various papers have been published on the phenomenon of stereocomplexation between i- and s-PMMA, a concept introduced by Liquori et al.[2] Nevertheless the process is still not completely understood. Vorenkamp et al. proved the complexation stoichiometry to be 1 i-unit:2 s-units at the level of monomeric units.[3] Bosscher et al. found that stereocomplexes were also formed when the methyl group of the ester of s-PMMA was replaced by an ethyl or even a *tert*-butyl group, while a modification of the ester group of i-PMMA prevented the formation of stereocomplexes.[4] On the grounds of these observations, conformational energy calculations, and fiber X-ray diffraction data they suggested for the structure of the stereocomplex a 30/4 i-helix surrounded by a 60/4 s-helix.[5]

Complexation is possible in bulk as well as in (dilute) solution. With respect to dilute solution three kinds of

0024-9297/88/2221-2195$01.50/0